

miR-19, miR-101 and miR-130 co-regulate ATXN1 levels to potentially modulate SCA1 pathogenesis

Yoontae Lee^{1,4}, Rodney C Samaco¹, Jennifer R Gatchel², Christina Thaller³, Harry T Orr⁵ & Huda Y Zoghbi¹⁻⁴

Spinocerebellar ataxia type 1 is caused by expansion of a translated CAG repeat in ataxin1 (ATXN1). The level of the polyglutamine-expanded protein is one of the factors that contributes to disease severity. Here we found that miR-19, miR-101 and miR-130 co-regulate ataxin1 levels and that their inhibition enhanced the cytotoxicity of polyglutamine-expanded ATXN1 in human cells. We provide a new candidate mechanism for modulating the pathogenesis of neurodegenerative diseases sensitive to protein dosage.

Polyglutamine (polyQ) diseases are dominantly inherited, neurodegenerative disorders that are caused by an expansion of CAG repeats that encode polyQ in the disease-causing protein¹⁻³. In all of these disorders, the polyQ-expanded proteins are toxic, leading to the degeneration of specific neurons. Although animal studies have shown that the levels of the mutant protein contribute to polyQ disease severity⁴⁻⁷, the *in vivo* mechanisms that regulate protein levels remain unknown.

To verify that mutant protein levels contribute to disease severity in the context of SCA1, we evaluated mice that overexpress *SCA1* (*ATXN1*) with 82 CAG repeats under the control of the Purkinje cell-specific *Pcp2* promoter (*SCA1*[82Q])⁴ in either the hemizygous or homozygous state. *SCA1*[82Q]^{Tg/Tg} mice show more severe motor impairment and Purkinje cell pathology than *SCA1*[82Q]^{Tg/+} mice (Supplementary Fig. 1 online). These data suggest that increased amounts of mutant protein result in a more severe disease.

Human *ATXN1* has a long 3' UTR (~7 kb), indicating that it might contain regulatory elements for post-transcriptional regulation (Fig. 1). One mechanism for regulating the amount of gene expression involves microRNAs (miRNAs), endogenous small noncoding RNAs that bind the 3' UTR of cognate target mRNAs to suppress their

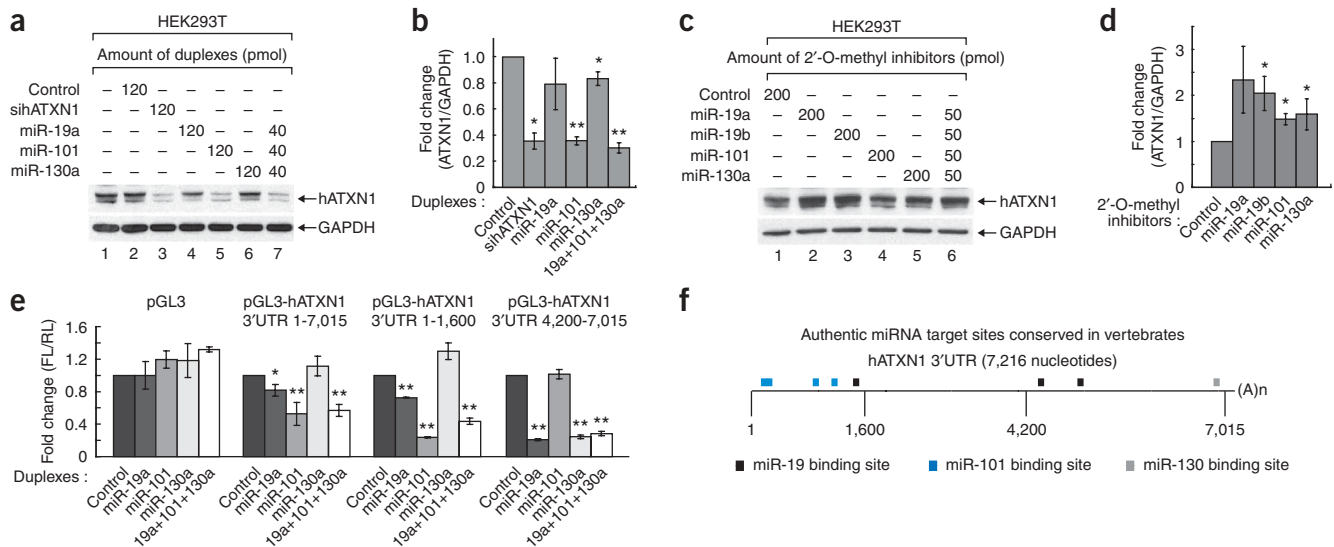


Figure 1 miR-19, miR-101 and miR-130 regulate ATXN1 levels. **(a,b)** miR-19a, miR-101 and miR-130a reduced the amount of ATXN1 in HEK293T cells. A representative western blot image **(a)** and the mean relative levels of ATXN1 (negative control = 1) and s.d. **(b)** are shown. **(c,d)** 2'-O-methyl inhibitors specific for each miRNA increased ATXN1 levels. Error bars represent s.d. **(e)** Luciferase assays using portions of the *ATXN1* 3' UTR, depicted by nucleotide number in the 3' UTR, identified the regions regulated by three different miRNAs. FL, firefly luciferase; RL, renilla luciferase. Error bars represent s.d. **(f)** Schematic of human *ATXN1* 3' UTR indicating the locations of the authentic miR-19, miR-101 and miR-130 target sites that are conserved in vertebrates and were verified by mutagenesis (Supplementary Figs. 6 and 7). * $P \leq 0.05$ and ** $P < 0.01$.

¹Department of Molecular and Human Genetics, Baylor College of Medicine, Houston, Texas 77030, USA. ²Departments of Neuroscience, ³Biochemistry and Molecular Biology and the ⁴Howard Hughes Medical Institute, Baylor College of Medicine, Houston, Texas 77030, USA. ⁵Institute of Human Genetics, Department of Biochemistry, Biophysics and Molecular Biology, Department of Laboratory Medicine and Pathology, University of Minnesota, Minneapolis, Minnesota 55455, USA. Correspondence should be addressed to H.Y.Z. (hzoghbi@bcm.tmc.edu).

Received 19 May; accepted 8 July; published online 31 August 2008; doi:10.1038/nn.2183

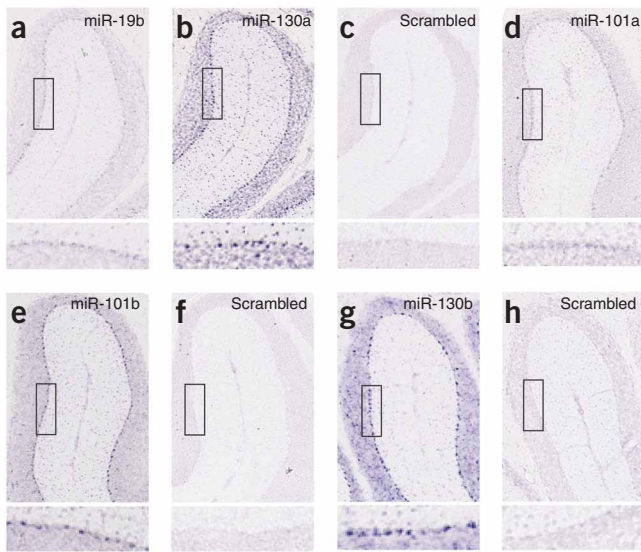


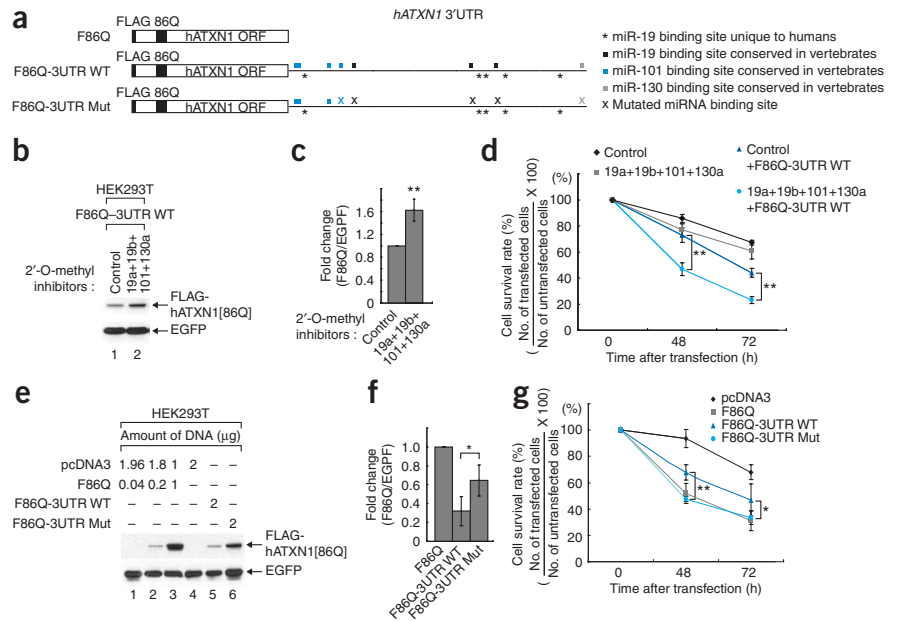
Figure 2 Purkinje cell expression of miR-19, miR-101 and miR-130. (a-h) *In situ* hybridization using locked nucleic acid probes for miR-19b (a), miR-130a (b), a scrambled control for miR-19b and miR-130a (c), miR-101a (d), miR-101b (e), a scrambled control for miR-101a and miR-101b (f), miR-130b (g) and a scrambled control for miR-130b (h). Upper panels show miR-19b, miR-101 and miR-130 expression in anterior cerebellar lobules and lower panels are enlarged images of boxed regions to show expression in Purkinje cells.

expression⁸. Notably, impairment of miRNA biogenesis in Purkinje cells results in cerebellar degeneration and ataxia in mice⁹. Thus, we hypothesized that miRNA-mediated post-transcriptional regulation of ATXN1 might modulate SCA1 neuropathology by affecting the amount of the protein expressed.

To test this hypothesis, we searched for evolutionarily conserved miRNA-binding sites in the 3' UTR of human *ATXN1* using miRNA target-prediction databases^{10,11}. Of the predicted miRNAs, we chose eight different miRNA candidates on the basis of the number of *ATXN1* target sites and their neuronal expression. To validate the role of the selected miRNAs in modulating *ATXN1* levels, we transfected MCF7 cells, which highly express endogenous *ATXN1* (Supplementary Fig. 2 online), with each miRNA duplex. miR-19a,

miR-101 and miR-130a downregulated *ATXN1* (Supplementary Fig. 2). Generally, different miRNAs act cooperatively on the same target mRNA to suppress its translation⁸. To determine whether this is the case for the miRNAs that we identified, we transfected different human cell lines (HEK293T, HeLa and MCF7 cells) with either each individual miRNA (miR-19a, miR-101 and miR-130a) or all of them combined. We observed a marked decrease in *ATXN1* levels on cotransfection of all three miRNAs; transfection of 120 pmol of each miRNA individually also decreased *ATXN1* levels (Fig. 1a,b and Supplementary Fig. 3 online). When we used 40 pmol of each individual miRNA, the reduction in *ATXN1* levels was less pronounced in comparison with 40 pmol of all three combined (Supplementary Fig. 3). Collectively, these data suggest that miR-19a, miR-101 and miR-130a cooperatively regulate *ATXN1* levels. Notably, only miR-101 affected both mRNA and protein levels, whereas miR-19a and miR-130a reduced the amount of protein without changing the amount of mRNA in HeLa cells (Supplementary Fig. 3). This suggests that miR-101 induces mRNA degradation as well as translational repression, whereas the others act primarily on translation. We also found that mouse *ATXN1* is cooperatively regulated by these three miRNAs (Supplementary Fig. 4 online), suggesting that the mechanism of *ATXN1* regulation by miR-19, miR-101 and miR-130 is conserved in mammals. When we used 2'-O-methyl inhibitors against miR-19, miR-101 and miR-130a, we found that *ATXN1* levels increased in HEK293T cells (Fig. 1c,d).

Figure 3 Inhibition of miRNA-mediated post-transcriptional regulation of polyQ-expanded *ATXN1* causes more severe cytotoxicity in HEK293T cells. (a) Schematic diagrams of three FLAG-hATXN1[86Q] constructs that either lacked the 3' UTR (F86Q), contained a wild-type 3' UTR (F86Q-3UTR WT) or contained a 3' UTR harboring mutated miRNA target sites (depicted by 'x', F86Q-3UTR Mut). ORF, open reading frame. (b,c) A mixture of 2'-O-methyl inhibitors specific for each miRNA (miR-19a, miR-19b, miR-101 and miR-130b) increased the amount of FLAG-hATXN1[86Q] expressed from F86Q-3UTR WT. A representative western blot image (b) and the mean relative levels of FLAG-hATXN1[86Q] (negative control = 1) and s.d. (c) are shown. We used enhanced green fluorescent protein (EGFP) as a normalization control for transfection efficiency. (d) Lethality was significantly enhanced in cells transfected with the mixture of 2'-O-methyl inhibitors specific for each miRNA and F86Q-3UTR WT compared with cells transfected with 2'-O-methyl inhibitor control and F86Q-3UTR WT. (e,f) Disruption of miRNA target sites in the *ATXN1* 3' UTR increased the amount of FLAG-hATXN1[86Q] that was present. A representative western blot image (e) and the mean relative levels of FLAG-hATXN1[86Q] (F86Q of lane 3 in the western image = 1) and s.d. (f) are shown. (g) Assays of cell viability 48 or 72 h after transfection with each vector indicate that there was significantly more lethality in cells expressing either F86Q or F86Q-3UTR Mut in comparison with cells expressing F86Q-3UTR WT. **P* ≤ 0.05 and ***P* < 0.01.



A representative western blot image (e) and the mean relative levels of FLAG-hATXN1[86Q] (F86Q of lane 3 in the western image = 1) and s.d. (f) are shown. (g) Assays of cell viability 48 or 72 h after transfection with each vector indicate that there was significantly more lethality in cells expressing either F86Q or F86Q-3UTR Mut in comparison with cells expressing F86Q-3UTR WT. **P* ≤ 0.05 and ***P* < 0.01.

To confirm that miR-19, miR-101 and miR-130 directly target the 3' UTR of *ATXN1*, we linked firefly luciferase reporter genes to partial or full-length human *ATXN1* 3' UTR (Supplementary Fig. 5) and carried out dual luciferase assays in HeLa cells. In the context of the full-length 3' UTR (pGL3-hATXN1 3' UTR 1–7,015), miR-101 markedly reduced reporter gene expression, whereas we observed only a marginal reduction with miR-19a and miR-130a, as compared with the pGL3 control (Fig. 1e). We observed marked suppression of two additional reporters containing the partial *ATXN1* 3' UTR in which miRNA target sites are enriched (pGL3-hATXN1 3' UTR 1–1,600 and 4,200–7,015), with a clear correlation between the number of putative target sites and the degree of downregulation (Fig. 1e). We then proceeded to identify the authentic miRNA target sites by mutagenizing each putative miRNA target site (except for the first miR-130 target site) conserved in vertebrates, as well as one miR-130 target site that is unique to humans (Supplementary Methods and Supplementary Figs. 6 and 7 online). Most of the conserved putative miRNA target sites, except for the fourth miR-19 target site and the miR-130 target site unique to humans, were authentic (Fig. 1f and Supplementary Figs. 6 and 7). Together, these data indicate that miR-19, miR-101 and miR-130 directly bind to the *ATXN1* 3' UTR to suppress the translation of *ATXN1*.

Cerebellar Purkinje cells are vulnerable in individuals with SCA1 and animal models where mutant *ATXN1* accumulates gradually and causes toxicity^{4,12,13}. To examine the possibility that the level of *ATXN1* could be regulated by miR-19, miR-101 and miR-130 in Purkinje cells, we investigated the expression pattern and level of these miRNAs in mouse cerebellum. Northern blot analysis demonstrated that they were expressed in the cerebellum (Supplementary Fig. 8 online) and RNA *in situ* hybridization revealed that miR-19b, miR-101 and miR-130 were expressed in Purkinje cells (Fig. 2). Of note, however, miR-101 and miR-130 were more abundant than miR-19 in Purkinje cells (Fig. 2), suggesting that miR-101 and miR-130 could dominantly act on *ATXN1* in this brain region. Altogether, the expression of these miRNAs in the cells most vulnerable in this disease suggests that they could be involved in modulating the toxicity of mutant *ATXN1*.

To investigate whether these miRNAs modulate the cytotoxicity of the polyQ-expanded *ATXN1*, we generated a polyQ-expanded *ATXN1* expression vector containing the wild-type 3' UTR of human *ATXN1* (F86Q-3UTR WT) and carried out a cell-based assay of mutant *ATXN1* toxicity (Supplementary Methods). We used HEK293T cells because the polyQ-expanded *ATXN1* induces cell death in this cell line¹⁴ and, more importantly, because molecular mechanisms that contribute to SCA1 pathogenesis in the cerebellum have been reproduced in this cell line in terms of the formation of the toxic protein complex containing the polyQ-expanded *ATXN1* and RBM17 (ref. 15). We tested whether inhibition of endogenous miR-19, miR-101 and miR-130 enhanced cytotoxicity of the polyQ-expanded *ATXN1* (hATXN1[86Q]) expressed from F86Q-3UTR WT. Inhibition of these three miRNAs increased hATXN1[86Q] levels (Fig. 3a–c). As a consequence, increased hATXN1[86Q] significantly reduced cell viability 48 and 72 h after transfection, in comparison with cotransfected F86Q-3UTR WT and control 2'-O-methyl inhibitor ($P < 0.01$), although a mixture of inhibitors specific for each miRNA (miR-19a, miR-19b, miR-101

and miR-130b) also induced slightly more cell death than the control inhibitor (Fig. 3d). To exclude the possibility that upregulation of other targets caused by inhibition of these miRNAs could contribute to a reduction in cell viability, we generated a hATXN1[86Q] expression vector containing the 3' UTR with mutated miRNA target sites (F86Q-3UTR Mut): three sites corresponding to miR-19 and a site corresponding to either miR-101 or miR-130 (Fig. 3a). Mutation of these particular miRNA target sites not only increased the level of hATXN1[86Q] but also reduced cell viability (Fig. 3e–g). These data suggest that the inhibition of miRNA-mediated post-transcriptional regulation of mutant *ATXN1* enhances its cytotoxicity.

In this study, we provide evidence for a previously unknown key regulatory mechanism by discovering miRNAs that regulate the level of a polyQ disease causing protein in mammals and demonstrate the modulatory role of miRNA-mediated mechanisms in *ATXN1* toxicity. The identification of this new modulatory pathway of *ATXN1* begs the question of whether similar regulatory mechanisms exist for other polyQ proteins and for proteins implicated in neurodegenerative diseases that are caused by a gain-of-function mechanism and are sensitive to disease protein levels. Moreover, such findings raise the possibility that mutations in the miRNA-binding sites or the miRNA genes themselves might cause neurodegenerative phenotypes owing to an accumulation of *ATXN1*.

Note: Supplementary information is available on the Nature Neuroscience website.

ACKNOWLEDGMENTS

We thank N. Ao, Y. Liu and A. Liang of the Baylor College of Medicine *In Situ* Hybridization core for technical assistance and V.N. Kim and members of the Zoghbi laboratory for helpful discussions and comments on the manuscript. This research was supported by US National Institutes of Health grants NS27699 and HD24064 to H.Y.Z. and NS22920 to H.T.O. H.Y.Z. is an investigator with the Howard Hughes Medical Institute.

AUTHOR CONTRIBUTIONS

Y.L. and H.Y.Z. designed the experiments. Y.L. carried out the majority of the experiments, with the exception of those comparing SCA1[82Q]^{Tg/Tg} and SCA1[82Q]^{Tg/Tg} mice in Supplementary Figure 1 (J.R.G. and R.C.S.) and the RNA *in situ* hybridization experiments in Figure 2 (C.T.). Data analyses and interpretation were conducted by Y.L., H.T.O. and H.Y.Z. Y.L. and H.Y.Z. wrote the paper.

Published online at <http://www.nature.com/natureneuroscience/>
Reprints and permissions information is available online at <http://npg.nature.com/reprintsandpermissions/>

- Orr, H.T. & Zoghbi, H.Y. *Annu. Rev. Neurosci.* **30**, 575–621 (2007).
- Orr, H.T. *et al. Nat. Genet.* **4**, 221–226 (1993).
- Banfi, S. *et al. Nat. Genet.* **7**, 513–520 (1994).
- Burright, E.N. *et al. Cell* **82**, 937–948 (1995).
- Cemal, C.K. *et al. Hum. Mol. Genet.* **11**, 1075–1094 (2002).
- Xia, H. *et al. Nat. Med.* **10**, 816–820 (2004).
- Huynh, D.P., Figueroa, K., Hoang, N. & Pulst, S.M. *Nat. Genet.* **26**, 44–50 (2000).
- Bartel, D.P. *Cell* **116**, 281–297 (2004).
- Lewis, B.P., Shih, I.H., Jones-Rhoades, M.W., Bartel, D.P. & Burge, C.B. *Cell* **115**, 787–798 (2003).
- Krek, A. *et al. Nat. Genet.* **37**, 495–500 (2005).
- Schaefer, A. *et al. J. Exp. Med.* **204**, 1553–1558 (2007).
- Zoghbi, H.Y. & Orr, H.T. *Semin. Cell Biol.* **6**, 29–35 (1995).
- Clark, H.B. *et al. J. Neurosci.* **17**, 7385–7395 (1997).
- Rich, T. & Varadaraj, A. *PLoS ONE* **2**, e1014 (2007).
- Lim, J. *et al. Nature* **452**, 713–718 (2008).